

1 **Evolution of a fatty acyl-CoA elongase underlies desert adaptation in *Drosophila***

2

3

4 Zinan Wang^{1,2,5}, Jian Pu^{1,3,5}, Cole Richards¹, Elaina Giannetti¹, Haosu Cong¹, Zhenguo Lin⁴, and Henry
5 Chung^{1,2,6}

6

7 ¹Department of Entomology, Michigan State University, East Lansing, MI 48824, USA

8 ²Ecology, Evolution, and Behavior Program, Michigan State University, East Lansing, MI 48824, USA

9 ³College of Agriculture, Sichuan Agricultural University, Chengdu, Sichuan 611130, China

10 ⁴Department of Biology, Saint Louis University, St. Louis, MO 63104, USA

11 ⁵These authors contributed equally

12 ⁶To whom correspondence may be addressed. Email: (hwchung@msu.edu)

13

14 **Keywords:** Cuticular hydrocarbons, CRISPR/Cas9, desiccation resistance, *Drosophila mojavensis*

15

16 **Short title:** Evolution in *mElo* underlies desert adaption in *Drosophila*

17 **ABSTRACT**

18 To survive in extreme environments such as hot-arid deserts, desert-dwelling species have evolved
19 physiological traits to withstand the high temperatures and low aridity beyond the physiologically tolerable
20 ranges of most species. Such traits which include reducing water loss have independently evolved in
21 multiple taxa. However, the genetic and evolutionary mechanisms underlying these traits have thus far not
22 been elucidated. Here we show that *Drosophila mojavensis*, a fruitfly species endemic to the Sonoran and
23 Mojave deserts, had evolved extremely high desiccation resistance, by producing very long chained methyl-
24 branched cuticular hydrocarbons (mbCHCs) that contributes to a cuticular waterproofing lipid layer reducing
25 water loss. We show that the ability to synthesize these longer mbCHCs is due to evolutionary changes in
26 a fatty acyl-CoA elongase (*mElo*). CRISPR/Cas9 knockout of *mElo* in *D. mojavensis* led to loss of longer
27 mbCHC production and significant reduction of desiccation resistance at high temperatures but did not
28 affect mortality at high temperatures or desiccating conditions individually, indicating that this gene is crucial
29 for desert adaptation. Phylogenetic analysis showed that *mElo* is a *Drosophila* specific gene with no clear
30 ortholog outside Diptera. This suggests that while the physiological mechanisms underlying desert
31 adaptation are general, the genetic mechanisms may be lineage-specific.

32 INTRODUCTION

33 The divergence and evolution of adaptive traits allows organisms to survive and thrive in diverse and
34 extreme environments (Bardgett and Van Der Putten, 2014; McDonnell and Hahs, 2015; Rahbek et al.,
35 2019). A key feature of these extreme environments is having multiple abiotic factors of which levels are
36 beyond the physiologically tolerable ranges of most species (Hofmann and Todgham, 2010). In many cases,
37 the interaction between abiotic factors may exacerbate the stresses caused by these factors to organisms
38 that live in the environments (Filazzola et al., 2021; Mittler, 2006; Zhang et al., 2022). For example, in hot-
39 arid deserts, the increased organismal water loss due to high vapor pressure deficit caused by high levels
40 of aridity is exacerbated by high temperatures leading to even more rapid water loss (Cloudsley-Thompson,
41 1975; Gibbs et al., 1998). Nevertheless, species that are able to survive in these environments had evolved
42 traits that allow them to withstand these stresses.

43 To survive rapid water loss in deserts, species from different taxa evolved high levels of desiccation
44 resistance *via* similar physiological changes such as reducing water evaporation from the body, lowering
45 metabolism, and minimizing water excretion (Gibbs, 2002; Merkt and Taylor, 1994; Williams and Tieleman,
46 2005). While there are some research on these independently evolved physiological traits (Gibbs and
47 Matzkin, 2001; Rocha et al., 2021a; Xu et al., 2020), the underlying molecular and evolutionary mechanisms
48 remain largely unknown. Recent association studies using genomic and transcriptomic studies have
49 identified some candidate genes that may contribute to physiological adaptation in desert organisms
50 (Gonzalez-Tokman et al., 2020; Rocha et al., 2021b; Wang et al., 2021), but the function of these genes
51 are not characterized. In addition, it is not clear whether these adaptive traits in diverse desert species
52 share the underlying same genetic mechanisms or are specific to different lineages of species. Determining
53 the genetic basis underlying the evolution of desert adaptative traits may allow the prediction of whether
54 and how contemporary species will evolve and adapt to future environmental changes such as global
55 desertification (Huang et al., 2016; Shi et al., 2021).

56 In this study, we investigated the genetic basis underlying desert adaptation in a widely studied
57 desert species, *D. mojavensis* (Gibbs, 2002; Matzkin and Markow, 2009). This species has adapted to
58 several non-habitable deserts in southern California and Mexico (Reed et al., 2007), such as the Sonoran
59 Desert where the relative humidity in the summer can be lower than 10% and the air temperature routinely
60 exceeds 40°C (Gibbs et al., 2003). *D. mojavensis* has one of the highest levels of desiccation resistance
61 (Kellermann et al., 2012) and the lowest rate of water loss in desiccating environments among *Drosophila*
62 species (Gibbs and Matzkin, 2001). We showed that the high desiccation resistance of *D. mojavensis* at
63 these desert conditions is due to its ability to synthesize very long chained methyl-branched cuticular
64 hydrocarbons (mbCHCs), which contributes to a waterproofing lipid layer on its cuticle, reducing water loss.
65 The synthesis of these very long chained mbCHCs is due to coding differences in a fatty acyl-CoA elongase
66 (*mElo*) that allows *D. mojavensis* to synthesize longer mbCHCs compared to *D. melanogaster*, a well-
67 studied cosmopolitan species. Phylogenetic analyses showed that *mElo* is a lineage-specific gene in

68 *Drosophila* and two sibling genera in the same subfamily, suggesting that the evolution of *mElo* may
69 contribute to the adaptation to future warmer and drier environments in species of these genera.

70

71 RESULTS

72 **The fatty acyl-CoA elongase *mElo* (CG18609) elongates methyl-branched CHCs (mbCHCs) in *D.*** 73 ***melanogaster***

74 We had previously shown that the length of mbCHCs can largely explain desiccation resistance across
75 *Drosophila* species (Wang et al., 2022). *Drosophila* species produces combinations of mbCHCs of different
76 carbon backbone lengths ranging from 24 carbons (2MeC24) to 32 carbons (2MeC32) (Jallon and David,
77 1987; Khallaf et al., 2021; Wang et al., 2022). *D. melanogaster* mainly produces 2MeC24, 2MeC26, and
78 2MeC28, while *D. mojavensis* produces longer mbCHCs, 2MeC28, 2MeC30, and 2MeC32 (**Figure 1A**). As
79 CHCs are synthesized via the fatty acyl-CoA synthesis pathway, before decarbonylation to hydrocarbons
80 in insect oenocytes, we hypothesized that an oenocyte specific fatty acyl-CoA elongase may underlie
81 differences in the mbCHC chain lengths between these two species (Blomquist and Ginzl, 2021; Chung
82 and Carroll, 2015; Holze et al., 2021). A previous genome wide association study in *D. melanogaster*
83 showed that RNAi of a specific fatty acyl-CoA elongase, *CG18609*, reduces the production of mbCHCs
84 (Dembeck et al., 2015). To confirm the role of *CG18609* in the elongation of mbCHCs, we used
85 CRISPR/Cas9 to knock out this gene in *D. melanogaster*. While homozygous *CG18609* knockout strains
86 are viable and fertile, levels of 2MeC26 and 2MeC28 were significantly reduced (**Figure 1B**). Oenocyte-
87 specific GAL4/UAS expression of a *D. melanogaster CG18609* transgene in the homozygous knockout
88 strain was able to restore production of 2MeC26 and 2MeC28 (**Figure 1B**). This suggests that *CG18609* is
89 an elongase gene that is involved in the synthesis pathway of the fatty acyl-CoA precursors for 2MeC26
90 and 2MeC28 (**Figure 1C**). We named this gene *mElo* (***mb*CHC *E*longase**).

91

92 **Transgenic overexpression of the *D. mojavensis mElo* (*Dmoj/mElo*) gene in *D. melanogaster* leads** 93 **to longer mbCHC production and higher desiccation resistance**

94 To investigate the molecular mechanisms underlying longer mbCHCs in *D. mojavensis*, we focused on the
95 *mElo* gene of this species. At the *D. melanogaster mElo* locus, there are two elongase genes, *mElo* and
96 another elongase gene, *CG17821*, while the *mElo* locus in *D. mojavensis* contains four predicted elongase
97 genes, *GI20343*, *GI20344*, *GI20345*, and *GI20347* (**Figure 2A**). Phylogenetic analyses suggest that
98 *GI20347* is the ortholog of *mElo*, while *CG17821* is likely to be orthologous with *GI20343*, *GI20344* and
99 *GI20345* (**Figure S1**). We named *GI20347* as *Dmoj/mElo*. *In situ* hybridization with antisense probes of
100 these genes showed that *mElo* is expressed in adult *D. melanogaster* oenocytes, while *GI20343*, *GI20345*,
101 and *GI20347* (*Dmoj/mElo*) are expressed in adult *D. mojavensis* oenocytes. *CG17821* and *GI20344* are
102 not expressed in *D. melanogaster* and *D. mojavensis* oenocytes respectively (**Figure S2**).

103 To determine the function of these elongase genes in mbCHC production, we overexpressed *mElo*,
104 *GI20343*, *GI20345*, and *GI20347* individually in adult *D. melanogaster* oenocytes using the GAL4/UAS

105 system at 27°C. Overexpression of *GI20343* did not change mbCHC production in males but led to slightly
106 reduced 2MeC28 and increased 2MeC24 in females (**Figure 2B; Table S1**). The overexpression of *mElo*
107 in *D. melanogaster* led to an increase in 2MeC28 production and a decrease in 2MeC24 production, which
108 is similar to what we have shown in *mElo* homozygous knockout flies (**Figure 1B**). Overexpression of
109 *GI20343* and *GI20345* individually in the oenocytes altered proportions of 2MeC24, 2MeC26, and 2MeC28
110 produced but did not result in the production of any longer mbCHCs. However, when we overexpressed
111 *GI20347* (*Dmoj/mElo*), we observed a shift to the production of longer CHCs, including the increased
112 production of a longer mbCHC, 2MeC30, which is usually absent or present in trace amounts in *D.*
113 *melanogaster* (**Figure 2B**). As *GI20347* is the *D. mojavensis* ortholog of *D. melanogaster mElo*, we suggest
114 that protein coding differences in this elongase gene may underlie the differences in mbCHC production
115 between these two *Drosophila* species.

116 These overexpression strains allowed us to test our hypothesis that the production of longer
117 mbCHCs may confer higher desiccation resistance in *Drosophila* species, allowing species to survive in
118 desert conditions. To test this, we performed desiccation assays on the strains with *Dmel/mElo* and
119 *Dmoj/mElo* overexpression. Our experiments showed that transgenic *D. melanogaster* flies with *Dmoj/mElo*
120 overexpression were significantly more desiccation resistant (Mean \pm SE, Females: 13.0 \pm 0.3 h, Males:
121 7.8 \pm 0.2 h) compared to control flies (Females: 8.4 \pm 0.2 h, Males: 5.9 \pm 0.1 h) and flies with *Dmel/mElo*
122 overexpression (Females: 10.3 \pm 0.2 h, Males: 6.0 \pm 0.2 h) (**Figure 2C**). This result demonstrated that the
123 production of longer mbCHCs can significantly increase desiccation resistance, consistent with our previous
124 findings using synthetic mbCHCs (Wang *et al.*, 2022).

125

126 ***D. mojavensis mElo (Dmoj/mElo) confers high desiccation resistance at desert temperatures***

127 While our experiments showed that transgenic overexpression of *Dmoj/mElo* in *D. melanogaster* produces
128 longer mbCHCs such as 2MeC30 and confers significantly higher desiccation resistance, we did not
129 recapitulate the production of 2MeC32 and the very high desiccation resistance in the desert dwelling *D.*
130 *mojavensis* (Wang *et al.*, 2022). To investigate the role of *Dmoj/mElo* in mbCHC synthesis and desiccation
131 resistance in *D. mojavensis*, we used CRISPR/Cas9 to knockout *Dmoj/mElo* in *D. mojavensis*. Three
132 independent *Dmoj/mElo* knockout strains, M3.5, M3.9, and M3.11, carrying a 5-bp insertion, 90-bp deletion,
133 and 10-bp deletion in the exon 3 of *Dmoj/mElo*, respectively, were obtained (**Figure 3A, Figure S3**). All
134 three mutant strains are homozygous viable. We also established three independent isofemale strains,
135 ISO1, ISO2, and ISO3, from the parental population as controls.

136 In all three *Dmoj/mElo* knockout strains, 2MeC32, the longest mbCHC in *D. mojavensis*, was
137 reduced to trace amounts and 2MeC30 was significantly reduced compared to the control strains (**Figure**
138 **3B, Figure S4, Table S2**), suggesting that *Dmoj/mElo* is responsible for elongating 2MeC28 to 2MeC30
139 and 2MeC32 in *D. mojavensis*. We further examined how these changes in mbCHC lengths could affect
140 desiccation resistance of *D. mojavensis* by subjecting all knockout and control strains to the desiccation
141 assay at 27°C. However, we did not observe any significant difference in desiccation resistance between

142 the knockout strains and the controls at this temperature (**Figure 3C**). As the capability of CHCs in
143 preventing water loss is associated with their melting temperatures (Gibbs, 2007; Wigglesworth, 1945), and
144 the air temperature of the microhabitat of *D. mojavensis* (e.g., outside cactus necrosis in the Sonoran Desert)
145 is higher than 35 °C (Gibbs *et al.*, 2003), we considered the hypothesis that at these higher temperatures,
146 longer mbCHCs such as 2MeC32 may make a difference in desiccation resistance. Therefore, we tested
147 whether the reduced 2MeC30 and 2MeC32 in *Dmoj/mElo*-knockout *D. mojavensis* could affect its
148 desiccation resistance at 37°C, a temperature that is ecologically relevant to *D. mojavensis*.

149 Desiccation experiments at 37°C showed that across the board, time to mortality is faster than
150 experiments performed at 27°C. At this temperature, the three *Dmoj/mElo* knockout strains are significantly
151 less desiccation resistant (Females: 7.7 ± 0.2 h, Males: 8.9 ± 0.2 h) compared to the control strains
152 (Females: 18.0 ± 0.4 h, Males: 18.6 ± 0.4 h) (**Figure 3D**), suggesting that the production of longer mbCHCs
153 such as 2MeC30 and 2MeC32 is crucial in desiccation resistance in hot and dry conditions. To exclude the
154 possibility that the higher mortality of the *Dmoj/mElo* knockout flies compared to the control flies was due
155 to heat stress rather than increased water loss at 37°C, we tested the survival of adults of both knockout
156 and control strains at 37°C under a non-desiccating experimental environment (flies are given fresh food
157 every 2-3 days). Survival at 37°C between the control strains and the *Dmoj/mElo* knockout strains were not
158 significantly different under these conditions (**Figure S5**), suggesting that the increased mortality observed
159 during the desiccation experiment at 37°C was due to water loss rather than the higher temperature. Taken
160 together, our results demonstrated that in *D. mojavensis*, *Dmoj/mElo* underlies the production of long
161 mbCHCs such as 2MeC30 and 2MeC32 and contributes to the high desiccation resistance of this species
162 in its hot and arid desert environment.

163

164 **The *mElo* gene is a *Drosophila* specific mbCHC elongase**

165 As mbCHCs are almost ubiquitous in most insect species, we sought to investigate if the role of *Dmoj/mElo*
166 in determining mbCHC length and desiccation resistance is conserved across Insecta. Using the conserved
167 microsynteny (*Jabba*, *Cyp12b2*, *Hs3st-A*, *CG33998*, and *List*) around *CG17821* and *mElo* between *D.*
168 *melanogaster* and *D. mojavensis*, we investigated this locus 16 *Drosophila* species and five species from
169 closely related genera (*Scaptodrosophila*, *Chymomyza*, *Leucophenga*, *Phortica*, and *Ephydra*) (Kim *et al.*,
170 2021; Scott *et al.*, 2014; Vicoso and Bachtrog, 2015) (**Figure 4A**). We found that in the *Drosophila* species
171 examined, this microsynteny is conserved and the elongase gene copy number ranges from two to four
172 across these *Drosophila* species. This microsynteny is also conserved in *Scaptodrosophila lebanonensis*,
173 *Chymomyza costata*, and *Leucophenga varia*, and partially conserved in *Phortica variegata*, *Ephydra*
174 *gracilis*, and *Musca domestica*. There are two elongase genes at this locus in *S. lebanonensis* and *C.*
175 *costata*, but none in *L. varia*, *P. variegata*, and *E. gracilis*. This suggests that elongase genes at this locus
176 first originate in the common ancestor of the *Drosophila*, *Scaptodrosophila*, and *Chymomyza* genus (i.e.,
177 the *Drosophilinae* subfamily) (**Figure 4A**).

178 To determine the relationship of these elongase genes, we performed a phylogenetic analysis of
179 all these elongase genes at this locus from 16 *Drosophila* species, *S. lebanonensis*, and *C. costata*. We
180 also included elongase genes in *L. varia*, *P. variegata*, and *E. gracilis* which has the highest sequence
181 homology to the elongases at the *Drosophila mElo* locus. Phylogenetic analysis of all elongase genes in
182 *mElo* loci showed that each *Drosophila* species only has a single *mElo* ortholog (**Figure 4B**). In addition,
183 the elongase genes in *Scaptodrosophila* and *Chymomyza* did not cluster with those in *Drosophila* (**Figure**
184 **4B**), suggesting that the presence of multiple elongase genes in the two lineages is likely due to lineage-
185 specific gene duplication events. This result suggests that the *mElo* gene at the *Drosophila mElo* locus
186 originated in the genus *Drosophila*. However, this does not exclude the possibility that the *mElo* gene is
187 present in other insect species, but located in another genomic location, as mbCHCs are prevalent across
188 insect species. To determine if any *mElo* ortholog is present in other insect species, we compared elongase
189 genes *Aedes aegypti*, a Dipteran mosquito species and several non-Diptera species, *Apis mellifera*,
190 *Bombyx mori*, and *Tribolium castaneum*. From our phylogenetic analysis, we observed that while other
191 elongase genes such as *sit* and *CG31523* have 1:1 ortholog in all insect species, there is no clear *mElo*
192 orthologous gene identified (**Figure S6**). This suggests that *mElo* gene is a *Drosophila* specific mbCHC
193 elongase and other elongase genes may elongate mbCHCs in other insect species.

194

195 **DISCUSSION**

196 A few of the many species on Earth have evolved adaptive traits to live in extreme environments with harsh
197 abiotic conditions. However, few studies have determined the underlying genetic basis for such traits. In
198 this study, we show that the desert *Drosophila* species, *D. mojavensis*, has evolved coding changes in a
199 fatty acyl-CoA elongase gene, *mElo*, which led to the production of very long mbCHCs and high desiccation
200 resistance in this species. While the knockout of this gene in *D. mojavensis* has no significant effects on
201 desiccation resistance at a lower temperature (27°C), it significantly reduces desiccation resistance at a
202 higher temperature (37°C), which is within the average high temperature range in the Sonoran Desert
203 during summer (**Figure S7**). This suggests that these very long mbCHCs are able to reduce water loss at
204 hot-arid desert conditions i.e., high temperature and low humidity, and is crucial for survival in this habitat.
205 The transgenic overexpression of the *D. mojavensis mElo* gene in the cosmopolitan *D. melanogaster* led
206 to the production of longer mbCHCs and higher desiccation compared to the transgenic overexpression of
207 the *D. melanogaster mElo* gene, suggesting evolved coding differences in this gene between the two
208 species. Finally, phylogenetic analyses of this locus suggest that the *mElo* gene evolved recently and an
209 orthologous copy of this gene is not found outside Diptera.

210

211 **The very long mbCHCs in *D. mojavensis* are critical for survival in hot and arid deserts**

212 Why are there significant differences in desiccation resistance at 37°C but not at 27°C between *Dmoj/mElo*
213 knockout strains and the control strains? The ability of the CHC layer to prevent water loss depends on the
214 physical state of this solid-liquid mixture layer and this affects its ability to prevent water molecules from

215 diffusing through (Menzel et al., 2019). At a specific “phase transition” temperature, water loss through the
216 cuticle increases rapidly (Gibbs and Pomonis, 1995; Wigglesworth, 1945). This transition temperature is
217 determined by the CHC composition of each species (Gibbs and Pomonis, 1995; Menzel *et al.*, 2019).

218 We suggest that the loss of 2MeC32 and the significant decrease of 2MeC30 in the *Dmoj/mElo*
219 knockout strains altered the transition temperature of the CHC layer on *D. mojavensis*. At 27°C, this does
220 not affect the *Dmoj/mElo* knockout strains, therefore they do not differ significantly in desiccation resistance
221 from the control strains. However, at 37°C, *Dmoj/mElo* knockout strains begin to lose water more rapidly
222 than the control strains, resulting in a significant decrease in desiccation resistance compared to the control
223 strains (**Figure 5B**). As hot and arid deserts have long days of high temperatures during the summer, we
224 suggest that the very long mbCHCs in *D. mojavensis* are crucial for survival as they allow *D. mojavensis* to
225 survive the hot and dehydrating conditions during the long day before the dip in temperatures during the
226 night.

227

228 **Evolution at the *mElo* locus in *Drosophila***

229 The oenocyte driven overexpression of *Dmel/mElo* and *Dmoj/mElo* in the *D. melanogaster* produces
230 mbCHCs of different chain lengths (**Figure 2**), suggesting that there are differences in protein coding
231 sequences of this gene between the two *Drosophila* species, and that these differences contribute to the
232 different mbCHCs produced by these two species. Our previous study using ancestral trait reconstruction
233 showed that the last common ancestor of *D. melanogaster* and *D. mojavensis* has an mbCHC phenotype
234 that is intermediate between the mbCHCs phenotypes of the two species (Wang *et al.*, 2022). As *mElo*
235 controls the length of the longest mbCHCs produced in each of these two species, this suggests that
236 evolutionary changes in this gene may have occurred in both species from the common ancestor, i.e.,
237 evolution in this gene led to *D. melanogaster* to produce shorter mbCHCs and *D. mojavensis* to produce
238 longer mbCHCs as both species adapt to their environments (**Figure 5B**).

239 The CRISPR/Cas9 knockout of *mElo* in both species also produced different mbCHC phenotypes.
240 In *D. melanogaster*, knockout of *mElo* produced a mbCHC phenotype which is largely 2MeC24 in males
241 and 2MeC26 in females with significant decreases in 2MeC28 in both sexes compared to wild-type flies. In
242 *mElo* knockout *D. mojavensis*, while 2MeC30 and 2MeC32 are significantly reduced with the latter reduced
243 to trace amounts compared to wild-type flies, the major CHC in these *mElo* knockout *D. mojavensis* is still
244 2MeC30. This suggests that there are other elongase genes contributing to the mbCHC phenotype in *D.*
245 *mojavensis*. A candidate gene for this would be *GI20345*, another elongase gene in the *mElo* locus in *D.*
246 *mojavensis* that is expressed in *D. mojavensis* oenocytes and is able to elongate mbCHCs in *Dmel/mElo*
247 knockout *D. melanogaster* (**Figure 2**). This may suggest a complicated evolutionary scenario in the
248 evolution of mbCHC biosynthesis controlled by the *mElo* locus in *Drosophila* (**Figure S8**).

249

250 **Lineage specific genetic basis for the evolution of desiccation resistance**

251 Variations in CHC composition contribute to desiccation resistance differences across many insect species
252 (Buellesbach et al., 2018; Leeson et al., 2020; Rouault et al., 2004). While mbCHCs are found in almost all
253 insect species, our phylogenetic analyses showed that the *mElo* gene is a *Drosophila* specific mbCHC
254 elongase, indicating that the control of mbCHCs chain length in other species is likely to be a different
255 elongase gene. This suggests that contribution to the evolution of desiccation resistance and desert
256 adaptation by the *mElo* locus is likely to be lineage specific. If changes in CHC composition can contribute
257 to desiccation resistance in insects, what are the likely genetic mechanisms that underlie the evolution of
258 desiccation resistance beyond *Drosophila*? The CHC biosynthesis pathway is largely conserved in insects
259 and is made up of several fatty acyl-CoA synthesis gene families such as fatty acyl-CoA synthetases,
260 desaturases, fatty acyl-CoA reductases (FARs), and elongases (Blomquist and Ginzal, 2021). These gene
261 families evolved rapidly and contribute to the diversification of CHCs across insects (Finck et al., 2016;
262 Finet et al., 2019; Helmkampf et al., 2015; Tupec et al., 2019). Gains and losses of these genes as well as
263 changes in their oenocyte expression are likely to contribute to CHC changes and the evolution of
264 desiccation resistance in different insect species. The rapid “birth-and-death” of these genes also suggests
265 that many of the genetic mechanisms leading to CHC changes and the evolution of desiccation resistance
266 across different insect species are likely to be lineage specific.

267

268 **Conclusions**

269 In summary, we showed that evolutionary change in a fatty acyl-CoA elongase contributes to the adaptation
270 of *D. mojavensis* to the hot and arid Sonoran Desert by reducing water loss at a high temperature. While
271 the general mechanisms of CHC composition modification leading to reduction of water loss at high
272 temperatures in insects adapting to hotter and drier conditions are likely to be conserved, the specific
273 genetic mechanism is not. This may have implications in the prediction of species changes as climate
274 change continues to occur in the near future.

275

276 **ACKNOWLEDGEMENTS**

277 We thank Ye Ma, Mei Luo, and Taylor Hori for technical assistance, and Yuzhang Shan for assistance with
278 figure visualization. We acknowledge the Bloomington *Drosophila* Stock Center and National *Drosophila*
279 Species Stock Center for fly stocks. This work is supported by a National Science Foundation grant
280 (2054773) to H. Chung.

281

282 **AUTHOR CONTRIBUTIONS**

283 Z.W. and H. Chung designed research; Z.W., J.P., H. Cong, E.G., C.R., Z.L., and H. Chung performed
284 research; Z.W., Z.L., and H. Chung analyzed data; and Z.W. and H. Chung wrote the paper with input from
285 other authors.

286 **MATERIALS AND METHODS**

287 ***Drosophila* strains**

288 The *y w; attP40* strain was used for *in situ* hybridization and transgenesis in *D. melanogaster*. The *D.*
289 *mojavensis wrigleyi* strain (15081-1352.29) used was obtained from the National Drosophila Species Stock
290 Center (NDSSC). The *oenoGAL4* strain (*PromE(800) line 2M*) was a gift from Joel Levine (Billeter et al.,
291 2009). The balancer strain *w¹¹¹⁸; CyO/Sco; MKRS/TM6B, Tb¹* (#3703) and *y¹ w* P{y⁺t7.7=nos-*
292 *phiC31\int.NLS}X; CyO/Sco* (#34770) were obtained from the Bloomington *Drosophila* Stock Center. All
293 flies were maintained at room temperature on standard *Drosophila* food (Bloomington formulation, Genesee
294 Scientific). *D. melanogaster* GAL4/UAS experiments were performed at 27°C.

295

296 ***In situ* hybridization & Imaging**

297 *In situ* hybridization was performed on oenocytes of five-day-old adults using methods as described
298 previously (Chung et al., 2007; Pu et al., 2021). Primers that were used for synthesizing probes were listed
299 in **Table S4**. All *in situ* hybridization images were captured using the Nikon SMZ18 dissecting stereo
300 microscope system.

301

302 **Generation of *mElo* knockout by CRISPR/Cas9 genome engineering in *D. melanogaster***

303 CRISPR/Cas9-mediated homology-directed repair (HDR) was used to generate a knockout of *Dmel/mElo*.
304 The program, flyCRISPR Optimal Target Finder, was used to identify optimal CRISPR target sites (Gratz
305 et al., 2014). Target-specific sequences for *Dmel/mElo* were synthesized as oligonucleotides,
306 phosphorylated, annealed and ligated into the *BbsI* sites of *pU6-BbsI-chiRNA* (Addgene plasmid #45946)
307 (Gratz et al., 2013) (5': *Dmel/mElo-gRNA1-BbsI-F* and *Dmel/mElo-gRNA1-BbsI-R*, 3': *Dmel/mElo-gRNA2-*
308 *BbsI-F* and *Dmel/mElo-gRNA2-BbsI-R*). To construct the replacement donor, approximately 1kb homology
309 arms flanking the cut sites were amplified by PCR using primers *Dmel/mElo-RightHomo-AscI-F* and
310 *Dmel/mElo-RightHomo-XhoI-R* for the 5' homology arm and primers *Dmel/mElo-LeftHomo-EcoRI-F* and
311 *Dmel/mElo-LeftHomo-NotI-R* for the 3' homology. The replacement donors were cloned sequentially into
312 the corresponding cut sites of the dsDNA donor vector *pHD-DsRed-attP* (Addgene plasmid #51019). The
313 primers used for generating gRNA and replacement donor constructs are listed in **Table S4**. The two gRNA
314 constructs and the replacement donor construct were co-injected into the *w¹¹¹⁸; PBac{y⁺mDint2*
315 *GFPE.3xP3=vas-Cas9}VK00027* strain (denoted as *Cas9onIII* strain; BDSC #51324), which carries a *vasa-*
316 *Cas9* transgene on Chromosome 3. The dsRed fluorescence in the eyes was used to screen positive
317 progeny, which were then crossed to *w¹¹¹⁸* to remove the *vasa-Cas9* transgene before being back-crossed
318 for five generations and then made homozygous using the double balancer strain *w¹¹¹⁸; CyO/Sco;*
319 *MKRS/TM6B, Tb¹*. The replacement of *Dmel/mElo* with *attP/dsRED* by HDR was confirmed by PCR using
320 the primers *DmelCG18609-EcoRI-F* and *DmelCG18609-XbaI-R* and the presence of dsRed (**Figure S9A**).
321 The resulting strain is designated as *w¹¹¹⁸; CG18609^{KO-dsRED-attP} (mEloKO)*. A transgene carrying a *PhiC31*
322 integrase driven by a *nanos* enhancer was integrated into this strain by crossing it to *y¹,w*,P{y⁺t7.7=nos-*

323 *phiC31\int.NLS}X; Sco/CyO* (**Figure S9B**). The resulting strain is $w^{1118}, P\{y^{+7.7}=\text{nos-phiC31}\int.NLS}X;$
324 $CG18609^{KO-dsRED-attP}$ and named as the *mEloKOint* strain.

325

326 **Generation of plasmid constructs**

327 Primers used for generating all constructs are listed in **Table S4**. UAS overexpression constructs were
328 cloned in *PhiC-31* site-specific transformation vector, *pWalium10-MOE* (Ni et al., 2009). The genomic DNA
329 of *Dmel/CG17821*, *Dmel/CG18609* (*Dmel/mElo*), *Dmoj/GI20343*, *Dmoj/GI20344*, *Dmoj/GI20345*, and
330 *Dmoj/GI20347* (*Dmoj/mElo*) were amplified by PCR from genomic DNA of corresponding species and then
331 cloned into *pWalium10-MOE* vector using the *NdeI*, *EcoRI*, or *XbaI* sites. The *G5-GAL4* construct by cloning
332 the 5' regulatory region of *Dmoj/GI20345* into the GFP reporter vector *pS3aG* via the *AscI* and *SbfI* sites
333 (Williams et al., 2008). The GFP sequence was then cut out from this construct using *SpeI* and *SbfI* and
334 replaced with a GAL4 sequence *pBPGUw* (Addgene plasmid #17575) vector using *SpeI* and *SbfI*.

335

336 **Drosophila transgenesis and overexpression experiments**

337 Transgenesis in *D. melanogaster* (*y w; attP40* and *mEloKOint* strains) was performed using the *PhiC31*
338 integrase system following standard *Drosophila* transgenesis protocols. To generate overexpress UAS
339 strains, the overexpression constructs of elongase genes on *pWalium10-MOE* were individually injected
340 into the *y w; attP40* strain. The *G5-GAL4* construct and the overexpression construct of *Dmel/mElo* on
341 *pWalium10-MOE* were individually injected into the *mEloKOint* strain for the rescue of *mElo* expression in
342 *mElo* knockout *D. melanogaster*. All overexpression experiments were performed at 27°C by reciprocally
343 crossing *enoGAL4* strain (*enoGAL4* or *G5-GAL4*) and the corresponding UAS overexpression strain.

344

345 **Generation of *mElo* knockout by CRISPR/Cas9 genome engineering in *D. mojavensis***

346 To generate *Dmoj/mElo* mutant alleles in *D. mojavensis*, we used a non-homologous end joining mediated
347 strategy by injecting the mixture of Cas9 protein (#CP01; PNA Bio) and sgRNAs into the embryos of this
348 species. Following the protocol in Khallaf et al. (2020), we co-injected two sgRNAs targeting *Dmoj/white*
349 (*Dmoj/white_sgRNAa* and *Dmoj/white_sgRNAb*). *Dmoj/mElo* specific sgRNAs (*Dmoj/mElo_sgRNAa* and
350 *Dmoj/mElo_sgRNAb*) were designed using the online tool CRISPR Design (Gratz et al., 2013) and two
351 sgRNAs were selected. All sgRNAs were generated following the protocol in Kistler et al. (2015), with *in*
352 *vitro* transcription using T7 Megascript Kit (Ambion) and purification using a MegaClear Kit (Ambion).
353 Primers used for the synthesis of all sgRNAs were listed in **Table S4**. The final injection mixture is
354 composed of 300 ng/μL Cas9 protein and four sgRNAs, each 75 ng/μL. To screen for the offspring of *D.*
355 *mojavensis* carrying *Dmoj/mElo* mutant alleles, we used the T7E1 assay (NEB #E3321) to determine
356 potential mutations for every single fly following the protocol in (Zhu et al., 2019). To eliminate potential off-
357 targets from the gene knockout, all strains carrying mutations in *Dmoj/mElo* were backcrossed with the
358 parental *D. mojavensis* strain for at least five generations before being made homozygous.

359

360 **Cuticular hydrocarbon extraction and analyses**

361 CHC extraction, GC/MS analysis, CHC identification, and quantification were performed as described
362 previously (Wang *et al.*, 2022). The GC thermal program was set as follows: start from 100 °C, 5 °C/min
363 to 200 °C, and 3 °C/min to 325 °C. For each sex in each reciprocal cross, three extractions were conducted
364 as replicates and the results were pooled for further statistical analyses, so six replicates were performed
365 for each cross.

366

367 **Desiccation assay**

368 Desiccation assays were performed as described previously (Wang *et al.*, 2022). Silica gel (S7500-1KG)
369 was ordered from Sigma-Aldrich. For each genotype, six replicates were conducted, each three from each
370 reciprocal cross.

371

372 **Bioinformatics**

373 The sequences of all elongase genes used in this study were retrieved from the NCBI
374 (<http://www.ncbi.nlm.nih.gov>) database, VectorBase (Giraldo-Calderón *et al.*, 2015), and SilkDB
375 (Consortium, 2008) via TBLASTN using *CG17821* and *CG18609* as queries (Suppl. Fasta File). The DNA
376 or amino acid sequences were aligned with MUSCLE and manually adjusted for the phylogenetic
377 reconstruction using the maximum likelihood method in MEGA (Version 11) (Kumar *et al.*, 2018). The GTR
378 model with a Gamma distribution was applied to reconstruct phylogeny using CDS of elongase genes, while
379 the LG substitution matrix and a Gamma distribution with invariant sites (G+I) was applied using their amino
380 acid sequences. All phylogenetic reconstruction analyses used 1000 bootstrap replicates to test the
381 reliability of inferred trees. The phylogenetic relationship of *Drosophila* and related species used in this
382 study was adapted from (Finet *et al.*, 2021; Pu *et al.*, 2021).

383 REFERENCES

- 384 Bardgett, R.D., and Van Der Putten, W.H. (2014). Belowground biodiversity and ecosystem functioning.
385 Nature 515, 505-511.
- 386 Billeter, J.-C., Atallah, J., Krupp, J.J., Millar, J.G., and Levine, J.D. (2009). Specialized cells tag sexual and
387 species identity in *Drosophila melanogaster*. Nature 461, 987.
- 388 Blomquist, G.J., and Ginzl, M.D. (2021). Chemical Ecology, Biochemistry, and Molecular Biology of Insect
389 Hydrocarbons. Annual Review of Entomology 66, 45-60.
- 390 Buellesbach, J., Whyte, B.A., Cash, E., Gibson, J.D., Scheckel, K.J., Sandidge, R., and Tsutsui, N.D. (2018).
391 Desiccation resistance and micro-climate adaptation: cuticular hydrocarbon signatures of different
392 Argentine ant supercolonies across California. Journal of chemical ecology 44, 1101-1114.
- 393 Chung, H., Bogwitz, M.R., McCart, C., Andrianopoulos, A., Batterham, P., and Daborn, P.J. (2007). Cis-
394 regulatory elements in the Accord retrotransposon result in tissue-specific expression of the *Drosophila*
395 *melanogaster* insecticide resistance gene *Cyp6g1*. Genetics 175, 1071.
- 396 Chung, H., and Carroll, S.B. (2015). Wax, sex and the origin of species: Dual roles of insect cuticular
397 hydrocarbons in adaptation and mating. Bioessays 37, 822-830. 10.1002/bies.201500014.
- 398 Chung, H., Loehlin, D.W., Dufour, H.D., Vaccarro, K., Millar, J.G., and Carroll, S.B. (2014). A single gene
399 affects both ecological divergence and mate choice in *Drosophila*. Science 343, 1148-1151.
- 400 Cloudsley-Thompson, J.L. (1975). Adaptations of Arthropoda to arid environments. Annual review of
401 entomology 20, 261-283.
- 402 Consortium, I.S.G. (2008). The genome of a lepidopteran model insect, the silkworm *Bombyx mori*. Insect
403 Biochem. Mol. Biol. 38, 1036-1045.
- 404 Dembeck, L.M., Boroczky, K., Huang, W., Schal, C., Anholt, R.R., and Mackay, T.F. (2015). Genetic
405 architecture of natural variation in cuticular hydrocarbon composition in *Drosophila melanogaster*. eLife 4.
406 10.7554/eLife.09861.
- 407 Filazzola, A., Matter, S.F., and Maclvor, J.S. (2021). The direct and indirect effects of extreme climate
408 events on insects. Science of the Total Environment 769, 145161.
- 409 Finck, J., Berdan, E.L., Mayer, F., Ronacher, B., and Geiselhardt, S. (2016). Divergence of cuticular
410 hydrocarbons in two sympatric grasshopper species and the evolution of fatty acid synthases and
411 elongases across insects. Scientific reports 6, 1-13.
- 412 Finet, C., Kassner, V.A., Carvalho, A.B., Chung, H., Day, J.P., Day, S., Delaney, E.K., De Ré, F.C., Dufour,
413 H.D., and Dupim, E. (2021). DrosoPhyla: resources for drosophilid phylogeny and systematics. Genome
414 biology and evolution 13, evab179.
- 415 Finet, C., Slavik, K., Pu, J., Carroll, S.B., and Chung, H. (2019). Birth-and-death evolution of the fatty acyl-
416 CoA reductase (FAR) gene family and diversification of cuticular hydrocarbon synthesis in *Drosophila*.
417 Genome biology and evolution 11, 1541-1551.
- 418 Gibbs, A., and Pomonis, J.G. (1995). Physical properties of insect cuticular hydrocarbons: the effects of
419 chain length, methyl-branching and unsaturation. Comparative Biochemistry and Physiology Part B:
420 Biochemistry and Molecular Biology 112, 243-249.

- 421 Gibbs, A.G. (2002). Water balance in desert *Drosophila*: lessons from non-charismatic microfauna.
422 Comparative Biochemistry and Physiology Part A: Molecular & Integrative Physiology 133, 781-789.
- 423 Gibbs, A.G. (2007). Waterproof cockroaches: the early work of JA Ramsay. Journal of Experimental Biology
424 210, 921-922.
- 425 Gibbs, A.G., Louie, A.K., and Ayala, J.A. (1998). Effects of temperature on cuticular lipids and water balance
426 in a desert *Drosophila*: is thermal acclimation beneficial? The Journal of experimental biology 201, 71-80.
- 427 Gibbs, A.G., and Matzkin, L.M. (2001). Evolution of water balance in the genus *Drosophila*. Journal of
428 Experimental Biology 204, 2331-2338.
- 429 Gibbs, A.G., Perkins, M.C., and Markow, T.A. (2003). No place to hide: microclimates of Sonoran Desert
430 *Drosophila*. Journal of Thermal Biology 28, 353-362.
- 431 Giraldo-Calderón, G.I., Emrich, S.J., MacCallum, R.M., Maslen, G., Dialynas, E., Topalis, P., Ho, N., Gesing,
432 S., Consortium, V., and Madey, G. (2015). VectorBase: an updated bioinformatics resource for invertebrate
433 vectors and other organisms related with human diseases. Nucleic acids research 43, D707-D713.
- 434 Gonzalez-Tokman, D., Córdoba-Aguilar, A., Dáttilo, W., Lira-Noriega, A., Sánchez-Guillén, R.A., and
435 Villalobos, F. (2020). Insect responses to heat: physiological mechanisms, evolution and ecological
436 implications in a warming world. Biological Reviews 95, 802-821.
- 437 Gratz, S.J., Cummings, A.M., Nguyen, J.N., Hamm, D.C., Donohue, L.K., Harrison, M.M., Wildonger, J.,
438 and O'Connor-Giles, K.M. (2013). Genome engineering of *Drosophila* with the CRISPR RNA-guided Cas9
439 nuclease. Genetics 194, 1029-1035. 10.1534/genetics.113.152710.
- 440 Gratz, S.J., Ukken, F.P., Rubinstein, C.D., Thiede, G., Donohue, L.K., Cummings, A.M., and O'Connor-
441 Giles, K.M. (2014). Highly specific and efficient CRISPR/Cas9-catalyzed homology-directed repair in
442 *Drosophila*. Genetics 196, 961-971.
- 443 Helmkampf, M., Cash, E., and Gadau, J. (2015). Evolution of the insect desaturase gene family with an
444 emphasis on social Hymenoptera. Molecular biology and evolution 32, 456-471.
- 445 Hofmann, G.E., and Todgham, A.E. (2010). Living in the now: physiological mechanisms to tolerate a
446 rapidly changing environment. Annu Rev Physiol 72, 127-145.
- 447 Holze, H., Schrader, L., and Buellesbach, J. (2021). Advances in deciphering the genetic basis of insect
448 cuticular hydrocarbon biosynthesis and variation. Heredity 126, 219-234.
- 449 Huang, J., Yu, H., Guan, X., Wang, G., and Guo, R. (2016). Accelerated dryland expansion under climate
450 change. Nature Climate Change 6, 166-171.
- 451 Jallon, J.M., and David, J.R. (1987). Variations in cuticular hydrocarbons among the eight species of the
452 *Drosophila melanogaster* subgroup. Evolution 41, 294-302.
- 453 Kellermann, V., Loeschcke, V., Hoffmann, A.A., Kristensen, T.N., Fløjgaard, C., David, J.R., Svenning, J.C.,
454 and Overgaard, J. (2012). Phylogenetic constraints in key functional traits behind species' climate niches:
455 patterns of desiccation and cold resistance across 95 *Drosophila* species. Evolution 66, 3377-3389.
- 456 Khallaf, M.A., Auer, T.O., Grabe, V., Depetris-Chauvin, A., Ammagarahalli, B., Zhang, D.-D., Lavista-Llanos,
457 S., Kaftan, F., Weißflog, J., and Matzkin, L.M. (2020). Mate discrimination among subspecies through a
458 conserved olfactory pathway. Science advances 6, eaba5279.

- 459 Khallaf, M.A., Cui, R., Weißflog, J., Erdogmus, M., Svatoš, A., Dweck, H.K., Valenzano, D.R., Hansson,
460 B.S., and Knaden, M. (2021). Large-scale characterization of sex pheromone communication systems in
461 *Drosophila*. *Nature communications* 12, 1-14.
- 462 Kim, B.Y., Wang, J.R., Miller, D.E., Barmina, O., Delaney, E., Thompson, A., Comeault, A.A., Peede, D.,
463 D'Agostino, E.R., and Pelaez, J. (2021). Highly contiguous assemblies of 101 drosophilid genomes. *eLife*
464 10, e66405.
- 465 Kistler, K.E., Vosshall, L.B., and Matthews, B.J. (2015). A practical guide to genomeengineering with
466 CRISPR-Cas9 in the mosquito *Aedes aegypti*. *bioRxiv*.
- 467 Kumar, S., Stecher, G., Li, M., Knyaz, C., and Tamura, K. (2018). MEGA X: molecular evolutionary genetics
468 analysis across computing platforms. *Molecular biology and evolution* 35, 1547.
- 469 Leeson, S.A., Kennington, W.J., Evans, T.A., and Simmons, L.W. (2020). Phenotypic plasticity but no
470 adaptive divergence in cuticular hydrocarbons and desiccation resistance among translocated populations
471 of dung beetles. *Evolutionary Ecology* 34, 929-944.
- 472 Matzkin, L.M., and Markow, T.A. (2009). Transcriptional regulation of metabolism associated with the
473 increased desiccation resistance of the cactophilic *Drosophila mojavensis*. *Genetics* 182, 1279-1288.
- 474 McDonnell, M.J., and Hahs, A.K. (2015). Adaptation and adaptedness of organisms to urban environments.
475 *Annual review of ecology, evolution, and systematics* 46, 261-280.
- 476 Menzel, F., Morsbach, S., Martens, J.H., Räder, P., Hadjaje, S., Poizat, M., and Abou, B. (2019).
477 Communication versus waterproofing: the physics of insect cuticular hydrocarbons. *Journal of Experimental*
478 *Biology* 222.
- 479 Merkt, J.R., and Taylor, C.R. (1994). " Metabolic switch" for desert survival. *Proceedings of the National*
480 *Academy of Sciences* 91, 12313-12316.
- 481 Mittler, R. (2006). Abiotic stress, the field environment and stress combination. *Trends in plant science* 11,
482 15-19.
- 483 Ni, J.-Q., Liu, L.-P., Binari, R., Hardy, R., Shim, H.-S., Cavallaro, A., Booker, M., Pfeiffer, B.D., Markstein,
484 M., and Wang, H. (2009). A *Drosophila* resource of transgenic RNAi lines for neurogenetics. *Genetics* 182,
485 1089-1100.
- 486 Pu, J., Wang, Z., Cong, H., Chin, J.S., Justen, J., Finet, C., Yew, J.Y., and Chung, H. (2021). Repression
487 precedes independent evolutionary gains of a highly specific gene expression pattern. *Cell reports* 37,
488 109896.
- 489 Rahbek, C., Borregaard, M.K., Antonelli, A., Colwell, R.K., Holt, B.G., Nogues-Bravo, D., Rasmussen, C.M.,
490 Richardson, K., Rosing, M.T., and Whittaker, R.J. (2019). Building mountain biodiversity: Geological and
491 evolutionary processes. *Science* 365, 1114-1119.
- 492 Reed, L., Nyboer, M., and Markow, T. (2007). Evolutionary relationships of *Drosophila mojavensis*
493 geographic host races and their sister species *Drosophila arizonae*. *Molecular Ecology* 16, 1007-1022.
- 494 Rocha, J.L., Brito, J.C., Nielsen, R., and Godinho, R. (2021a). Convergent evolution of increased urine-
495 concentrating ability in desert mammals. *Mammal Review* 51, 482-491.
- 496 Rocha, J.L., Godinho, R., Brito, J.C., and Nielsen, R. (2021b). Life in deserts: the genetic basis of
497 Mammalian desert adaptation. *Trends in Ecology & Evolution* 36, 637-650.

- 498 Rouault, J.-D., Marican, C., Wicker-Thomas, C., and Jallon, J.-M. (2004). Relations between cuticular
499 hydrocarbon (HC) polymorphism, resistance against desiccation and breeding temperature; a model for
500 HC evolution in *D. melanogaster* and *D. simulans*. In *Drosophila melanogaster, Drosophila simulans: So*
501 *Similar, So Different*, (Springer), pp. 195-212.
- 502 Scott, J.G., Warren, W.C., Beukeboom, L.W., Bopp, D., Clark, A.G., Giers, S.D., Hediger, M., Jones, A.K.,
503 Kasai, S., and Leichter, C.A. (2014). Genome of the house fly, *Musca domestica* L., a global vector of
504 diseases with adaptations to a septic environment. *Genome biology* *15*, 1-17.
- 505 Shi, H., Tian, H., Lange, S., Yang, J., Pan, S., Fu, B., and Reyer, C.P. (2021). Terrestrial biodiversity
506 threatened by increasing global aridity velocity under high-level warming. *Proceedings of the National*
507 *Academy of Sciences* *118*, e2015552118.
- 508 Tupec, M., Buček, A., Janoušek, V., Vogel, H., Prchalova, D., Kindl, J., Pavlíčková, T., Wenzelova, P., Jahn,
509 U., and Valterova, I. (2019). Expansion of the fatty acyl reductase gene family shaped pheromone
510 communication in Hymenoptera. *Elife* *8*, e39231.
- 511 Vicoso, B., and Bachtrog, D. (2015). Numerous transitions of sex chromosomes in Diptera. *PLoS biology*
512 *13*, e1002078.
- 513 Wang, Y., Ferveur, J.F., and Moussian, B. (2021). Eco-genetics of desiccation resistance in *Drosophila*.
514 *Biological Reviews*.
- 515 Wang, Z., Receveur, J.P., Pu, J., Cong, H., Richards, C., Liang, M., and Chung, H. (2022). Desiccation
516 resistance differences in *Drosophila* species can be largely explained by variations in cuticular
517 hydrocarbons. *eLife Under review*.
- 518 Wigglesworth, V.B. (1945). Transpiration through the cuticle of insects. *Journal of Experimental Biology* *21*,
519 97-114.
- 520 Williams, J.B., and Tieleman, B.I. (2005). Physiological adaptation in desert birds. *Bioscience* *55*, 416-425.
- 521 Williams, T.M., Selegue, J.E., Werner, T., Gompel, N., Kopp, A., and Carroll, S.B. (2008). The regulation
522 and evolution of a genetic switch controlling sexually dimorphic traits in *Drosophila*. *Cell* *134*, 610-623.
- 523 Xu, S., Wang, J., Guo, Z., He, Z., and Shi, S. (2020). Genomic convergence in the adaptation to extreme
524 environments. *Plant communications* *1*, 100117.
- 525 Zhang, H., Zhu, J., Gong, Z., and Zhu, J.-K. (2022). Abiotic stress responses in plants. *Nature Reviews*
526 *Genetics* *23*, 104-119.
- 527 Zhu, G.-H., Jiao, Y., Chereddy, S.C., Noh, M.Y., and Palli, S.R. (2019). Knockout of juvenile hormone
528 receptor, Methoprene-tolerant, induces black larval phenotype in the yellow fever mosquito, *Aedes aegypti*.
529 *Proceedings of the National Academy of Sciences* *116*, 21501-21507.
- 530
- 531

FIGURES

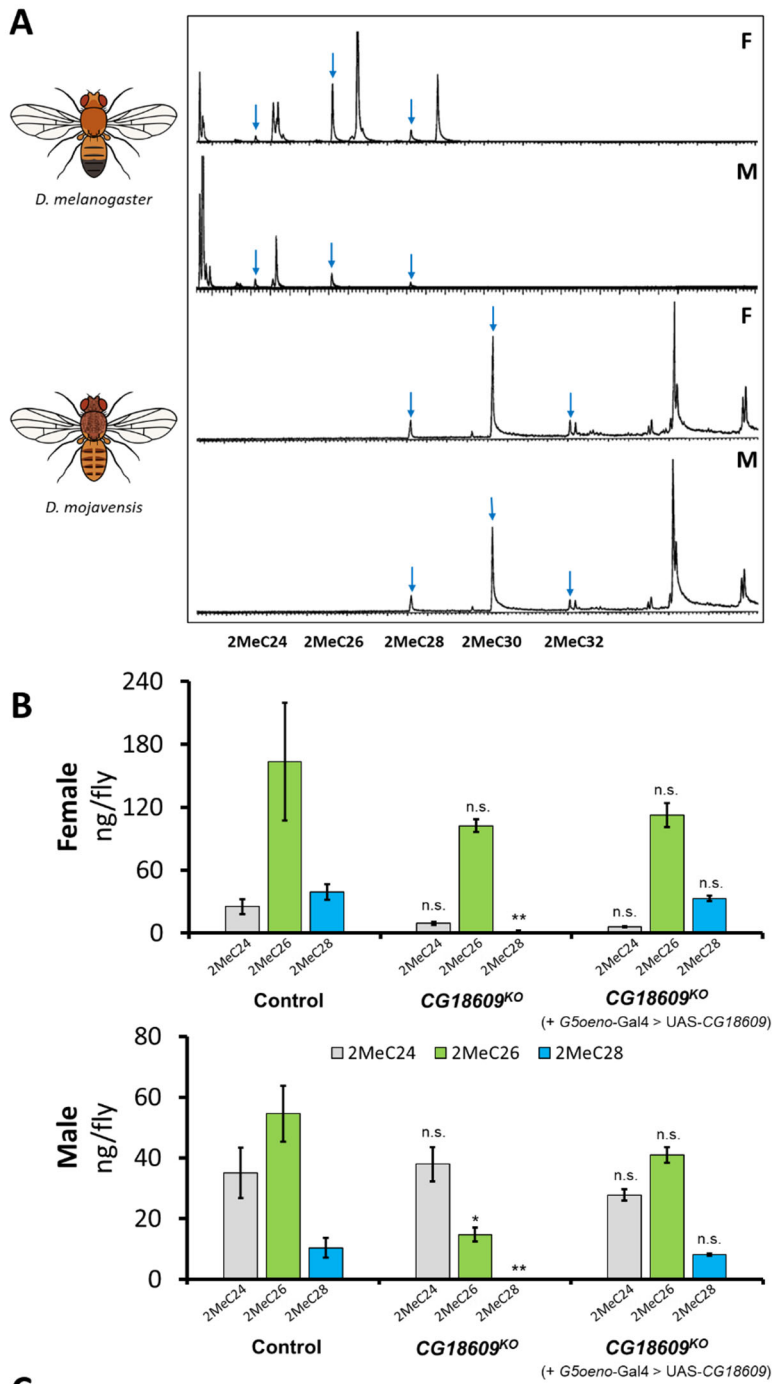


Figure 1. *mElo* (CG18609) is a methyl-branched CHCs (mbCHCs) elongase in *D. melanogaster*. (A)

Gas chromatography mass spectrometry (GC-MS) chromatograms showing male and female CHCs of *D. melanogaster* and *D. mojavensis*. The desert *Drosophila* species *D. mojavensis* produces longer mbCHCs than the cosmopolitan *D. melanogaster*. Blue arrows indicate mbCHCs in the chromatogram. **(B)** Levels of mbCHCs in *D. melanogaster* CG18609 homozygous knockout and rescue strains with oenocyte specific expression of CG18609 (*G5Oeno-Gal4>UAS-CG18609*) compared to the control strain *Cas9onIII*, which the knockout was derived from. In both sexes, the levels of 2MeC28 were significantly reduced (Welch t-test. Female: $t_{(4,1)} = 4.9$, $P = 0.007$; Male: $t_{(4)} = 3.2$, $P = 0.03$), while the level of 2MeC26 was only significantly reduced in males ($t_{(4,5)} = 4.2$, $P = 0.01$). No significant differences were observed in 2MeC24 in both sexes (Female: $P = 0.09$; Male: $P = 0.8$). The rescue strains were able to restore the production of mbCHCs in both sexes, leading to the same mbCHC profiles as shown in the control strain (2MeC24, Female: $P = 0.06$; Male: $P = 0.4$; 2MeC26, Female: $P = 0.4$; Male: $P = 0.2$; 2MeC28, Female: $P = 0.5$; Male: $P = 0.5$). **(C)** The role of CG18609 (*mElo*) in the elongation of 2MeC24 to 2MeC26 and 2MeC28 in *D. melanogaster*, based on knockout and rescue data.

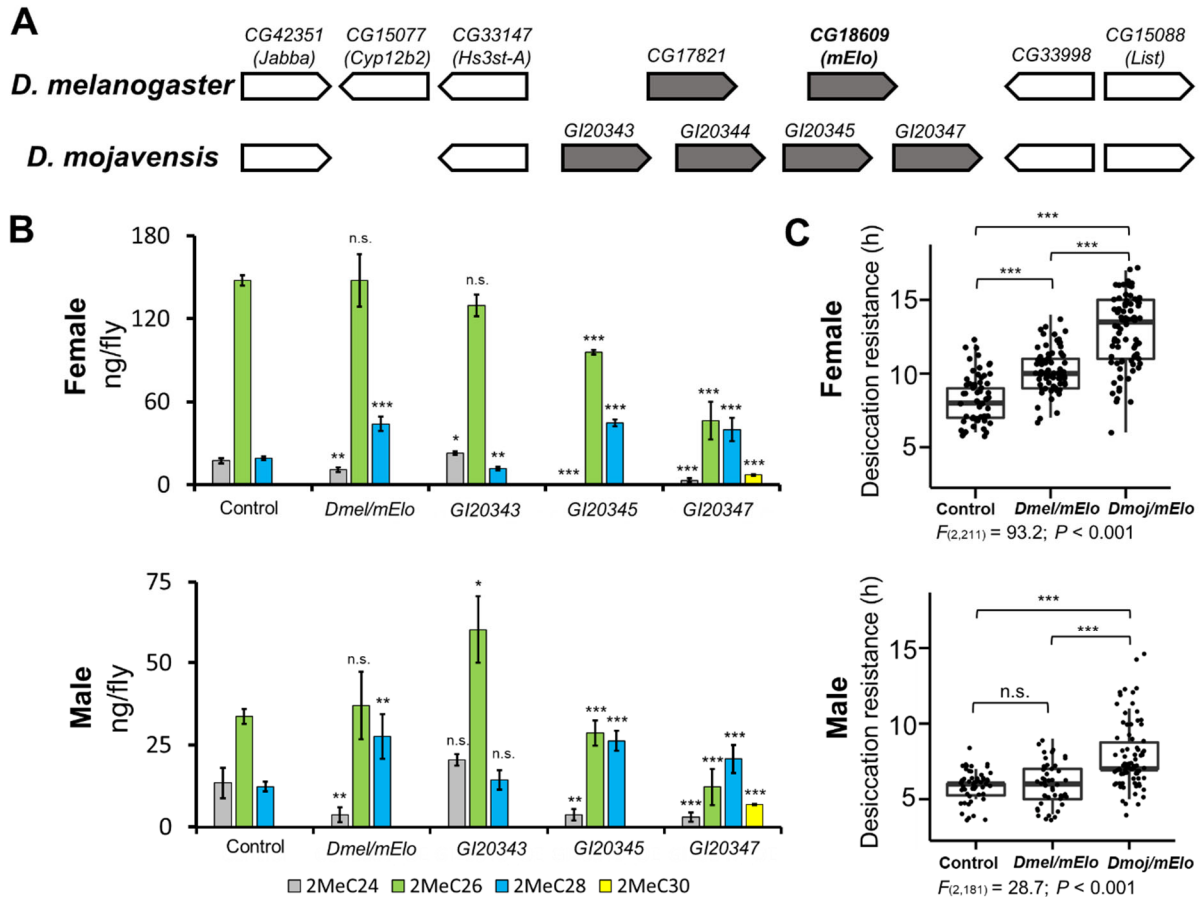


Figure 2. Oenocyte overexpression of *GI20347* in *D. melanogaster* leads to production of longer mbCHCs and confers higher desiccation resistance. (A) Microsynteny at the *mElo* locus is conserved between *D. melanogaster* and *D. mojavensis*. In *D. melanogaster*, two elongase genes, *CG17821* and *mElo* are present at this locus. In *D. mojavensis*, four elongase genes (*GI20343*, *GI20344*, *GI20345*, and *GI20347*) are present. **(B)** Quantities of mbCHCs (ng/fly) in *D. melanogaster* with each of the elongase genes (*mElo*, *GI20343*, *GI20345*, and *GI20347*) overexpressed in adult oenocytes using an oenocyte specific driver. The quantity of each mbCHC in the overexpression strains was compared with the control to determine any significant differences using the student's *t*-test at $\alpha=0.05$. **(C)** Desiccation resistance of *D. melanogaster* strains with *mElo* and *GI20347* (*Dmoj/mElo*) overexpressed in the oenocytes. Desiccation resistance is measured in hours (h) to mortality in a desiccating environment. Experiments were performed at 27°C for GAL4/UAS. Overexpression of *Dmoj/mElo* in *D. melanogaster* confers significantly higher desiccation resistance in both males and females compared to control strains or strains with overexpression of *Dmel/mElo*. One-way ANOVA was used to determine the differences in desiccation resistance between the strains of *D. melanogaster*, following with *post hoc* comparisons using Tukey's method. *: $P < 0.05$; **: $P < 0.01$; ***: $P < 0.001$.

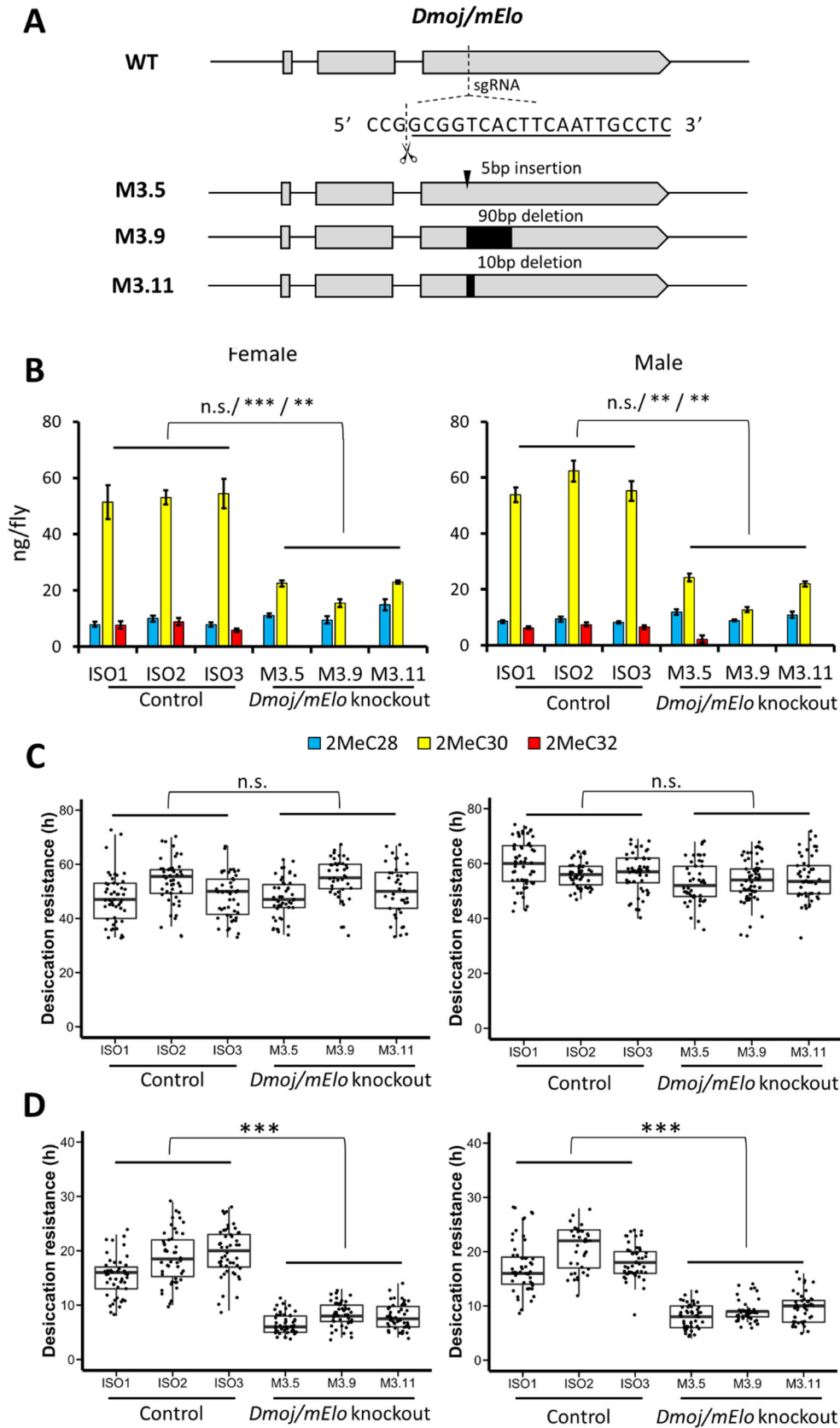


Figure 3. Knockout of the *mElo* ortholog *GI20347* (*Dmoj/mElo*) in *D. mojavensis* leads to a significant decrease in desiccation resistance at an ecologically relevant high temperature. (A) A CRISPR/Cas9 non-homologous end-joining strategy resulted in three homozygous viable strains with *Dmoj/mElo* knockout, M3.5, M3.9 and M3.11 in *D. mojavensis*, which have a 5 bp insertion, a 90 bp deletion, and a 10 bp deletion, respectively. **(B)** In the three *Dmoj/mElo* (*GI20347*) knockout strains, 2MeC30 was significantly reduced (~50% of wild type levels) and 2MeC32 is reduced to trace amounts (Female: 2MeC30: $t_{(4)} = -11.6$, $P < 0.001$, 2MeC32: $t_{(4)} = -8.5$, $P = 0.001$; Male: 2MeC30: $t_{(4)} = -8.5$, $P = 0.001$, 2MeC32: $t_{(4)} = -7.3$, $P = 0.002$). **(C)** There are no significant differences in desiccation resistance between the three *Dmoj/mElo* knockout strains and the three isofemale control strains at 27°C (Female: $P = 0.7$; Male: $P = 0.06$). **(D)** At 37°C, the three *Dmoj/mElo* knockout strains have a significant reduction in desiccation resistance compared to the three isofemale control strains (Female: $t_{(4)} = 7.4$, $P = 0.002$; Male: $t_{(4)} = 9.5$, $P < 0.001$). For both CHC quantities and desiccation resistance, linear mixed effects models were applied to compare the two groups of flies using 'lmer' function in R (ver 4.1). The three isofemale wild type and independent knockout strains were included as random effects. The difference between the wildtype and knockout flies was determined by paired contrast at $\alpha = 0.05$.

Figure 4. The origins of *mElo* in *Drosophila*. **(A)** The *mElo* loci in 16 *Drosophila* species and species from six closely related genera. The *mElo* loci were identified based on the conserved genes in the *D. melanogaster mElo* locus (*Jabba*, *Cyp12b2*, *Hs3st-A*, *CG33998*, and *List*) which are used as anchor genes in our analysis. All *Drosophila* species contains at least two elongase genes at this locus. There was an expansion of elongase genes in the virilis and repleta clades where species have 3-4 elongase genes at this locus (denoted by a *). Two elongase genes are present in *S. lebanonensis* and *C. costata*, but none in *L. varia*, *P. variegata*, and *E. gracilis*. This suggests that elongase genes at this locus first originated in the common ancestor of the *Drosophila*, *Scaptodrosophila*, and *Chymomyza* genus (denoted by a *). The dashed line indicates that anchor genes can be located in the genome but at different location. **(B)**. Phylogenetic relationship of elongase genes in *mElo* loci of Drosophilinae species as well as the elongases from *S. lebanonensis*, *C. costata*, *L. varia*, *P. variegata*, and *E. gracilis* that share the highest similarities to *mElo*. The phylogenetic tree was inferred by the ML method using amino acid sequences with 1000 bootstrap tests. The numbers next to nodes represent bootstrap values.

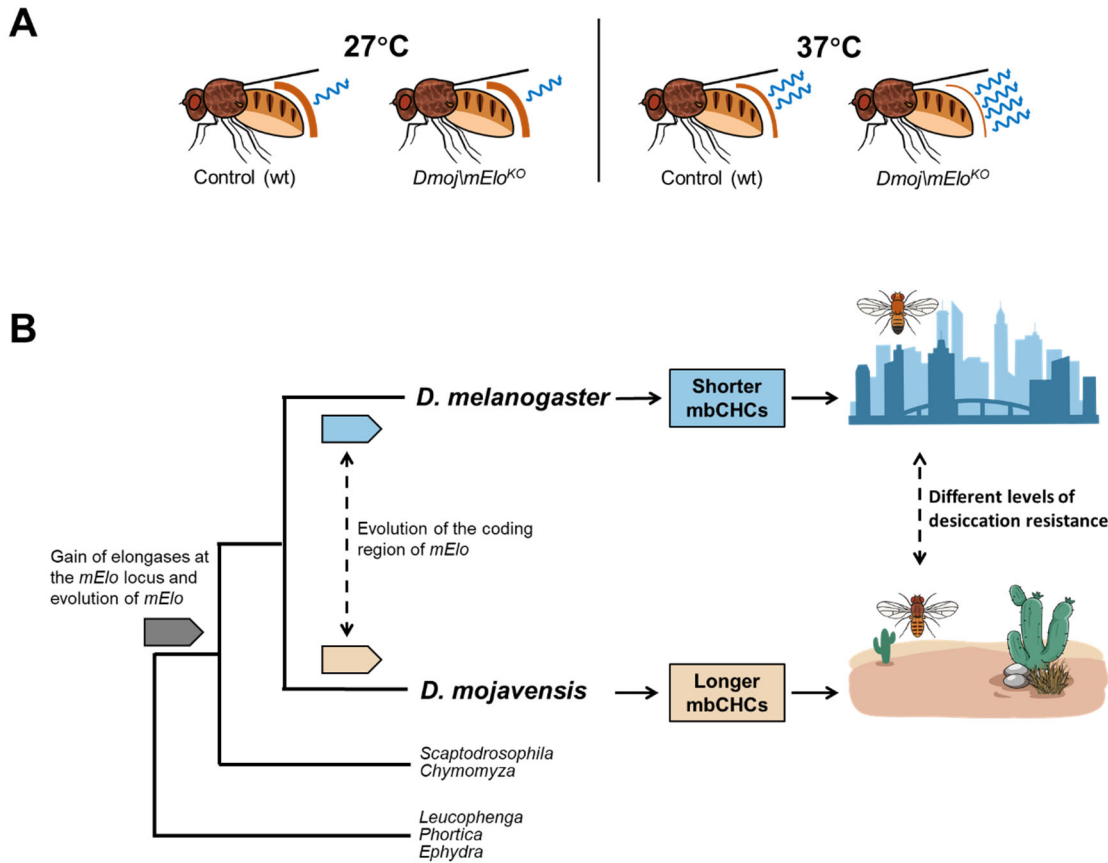


Figure 5. Evolution a fatty acyl-CoA elongase gene, *mElo*, underlie higher desiccation resistance and desert adaptation in *D. mojavensis*. (A) A schematic showing that the loss of 2MeC32 and a significant amount of 2MeC30 at 27°C does not affect the *Dmoj/mElo* strain of *D. mojavensis* compared to the control strain as water loss is similar between these strains. However, at the higher temperature of 37°C, we hypothesized the *Dmoj/mElo* strain loses water more rapidly compared to the control strain due to the melting temperatures of the CHC layer being altered by the loss of these longer mbCHCs. (B) A model showing how coding changes in *mElo* led to shorter mbCHCs in the cosmopolitan species *D. melanogaster* and longer mbCHCs in the desert species, *D. mojavensis*, allowing it to survive in the hot and dry desert.

SUPPLEMENTARY FIGURES

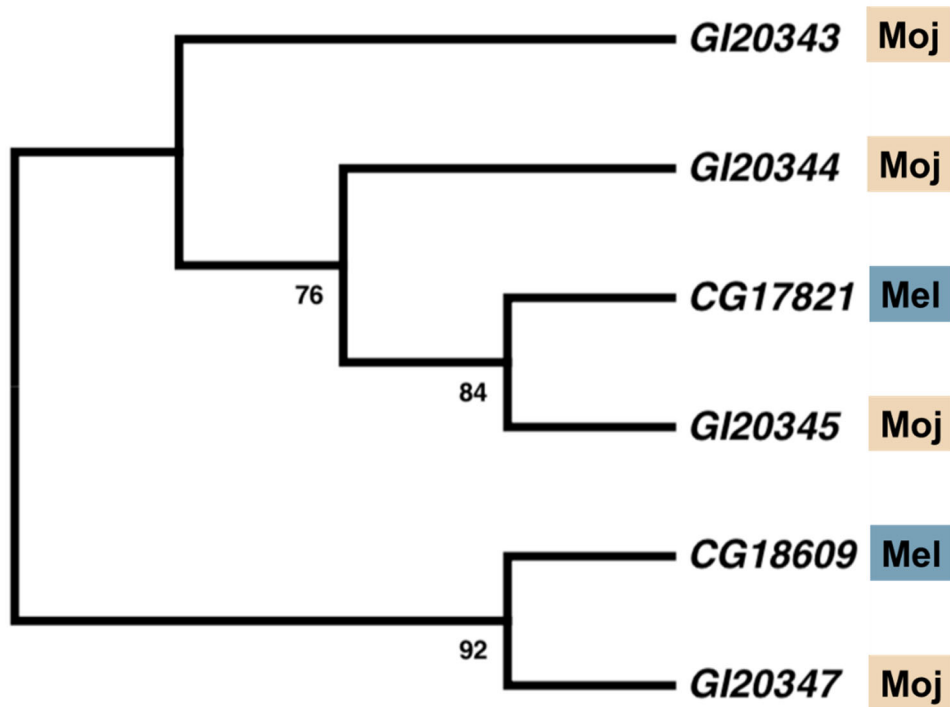


Figure S1. Phylogeny of elongases in the *mElo* loci of *D. melanogaster* and *D. mojavensis*. The coding sequences of these genes were used to generate the phylogeny using the Maximum Likelihood method with GTR model and 1000 bootstraps. The phylogenetic analysis showed that the *D. mojavensis* orthologue of *mElo* is *GI20347*.

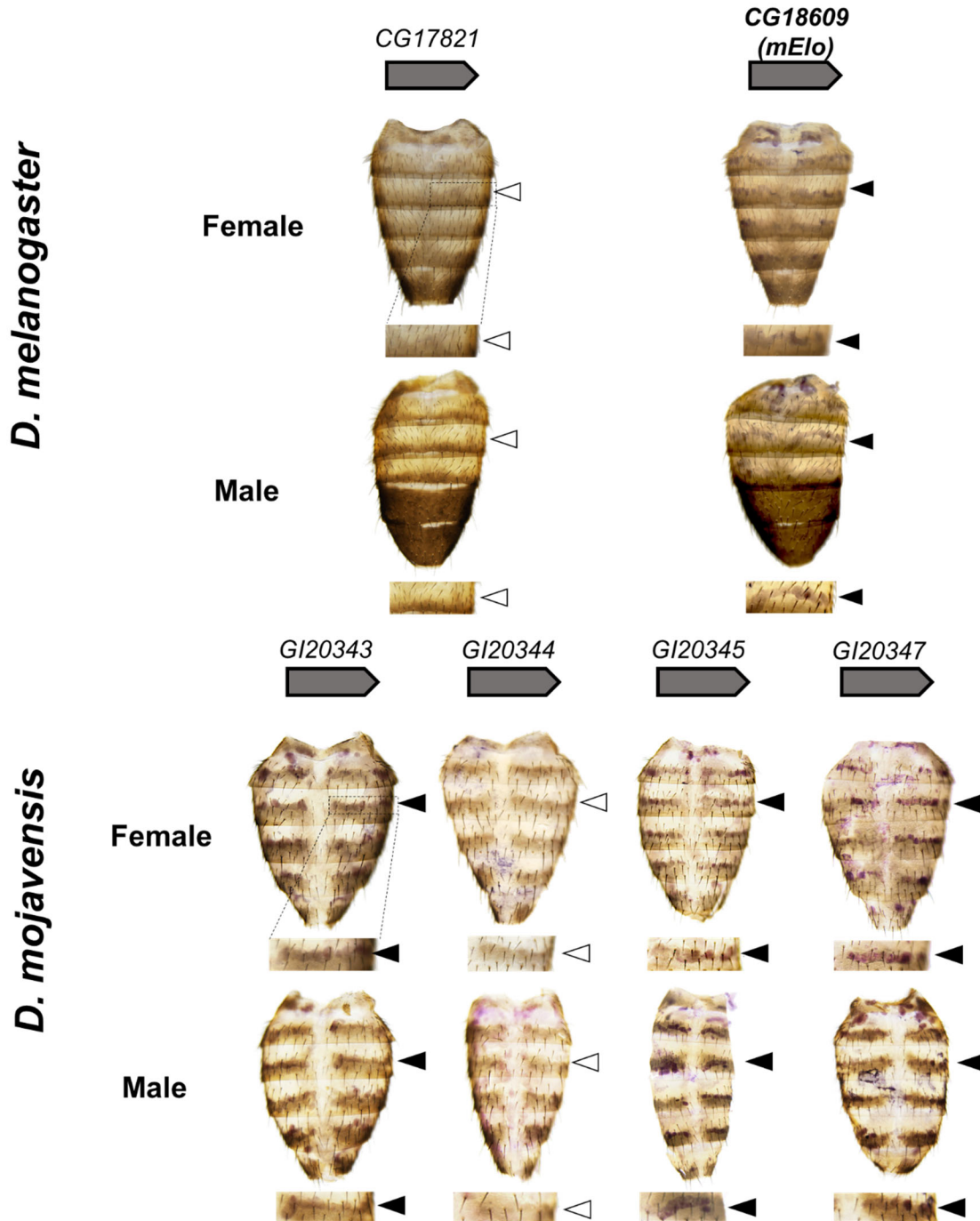


Figure S2. RNA *in situ* hybridization of fatty acyl-CoA elongase genes in the *D. melanogaster* and the *D. mojavensis* *mElo* loci on adults. In *D. melanogaster*, *CG18609* RNA transcript was detected in the adult oenocytes. In *D. mojavensis*, *G120343*, *G120345*, and *G120347* RNA transcripts were detected in the adult oenocyte. The expression of all the four genes are sexually monomorphic. Arrowheads point to oenocytes. Filled arrowheads indicate visible expression detected and open arrowheads indicate no visible expression.

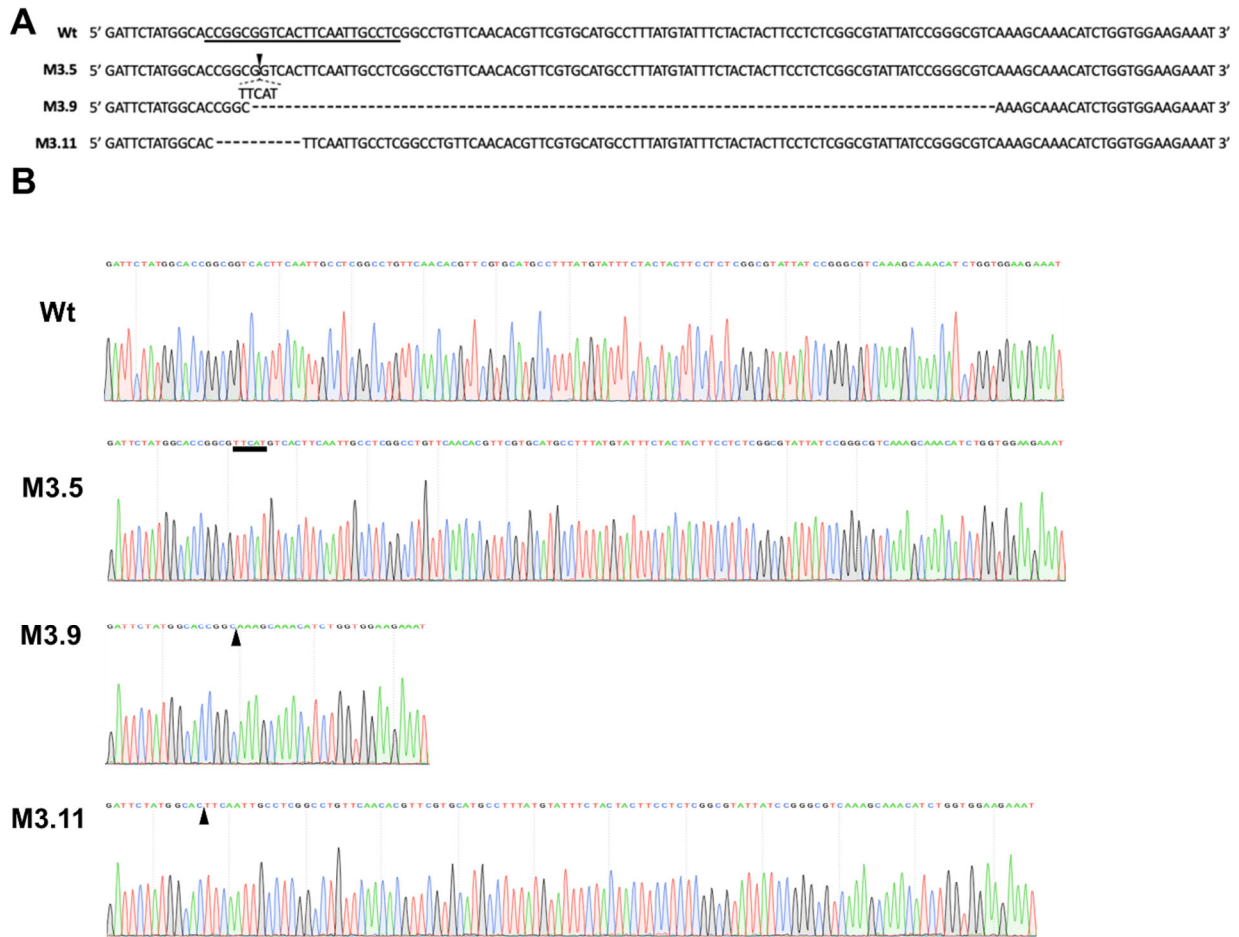


Figure S3. Edited sequences in M3.5, M3.9, and M3.11 strains. CRISPR/Cas9 and non-homologous end-joining was used to generate knockout strains of *G/20347*. Three independent knockout strains, namely M3.5, M3.9, and M3.11, were generated. They carry a 5-bp insertion, 90-bp deletion, and 10-bp deletion in the exon 3 of *Dmoj/mElo*, respectively.

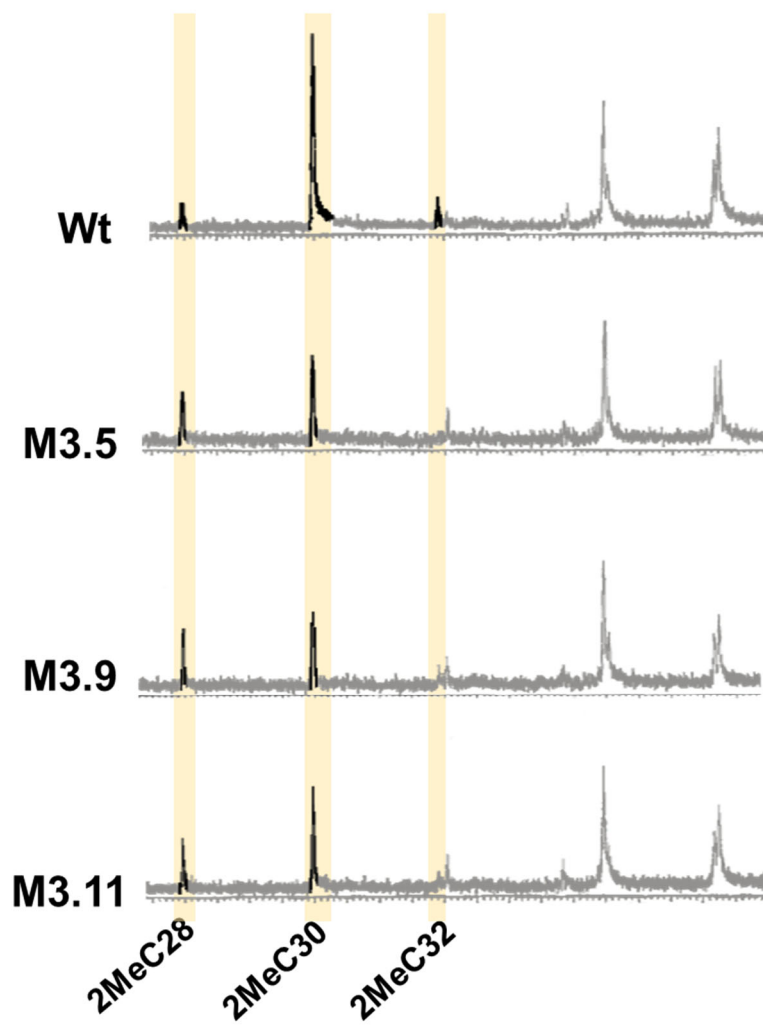


Figure S4. GC-MS chromatograms of mbCHCs in three homozygous *Dmoj/mElo* knockout strains of *D. mojavensis*, M3.5, M3.9 and M3.11. In all three knockout strains, levels of 2MeC30 and 2MeC32 were reduced and levels of 2MeC28 were increased compared to the wild-type control.

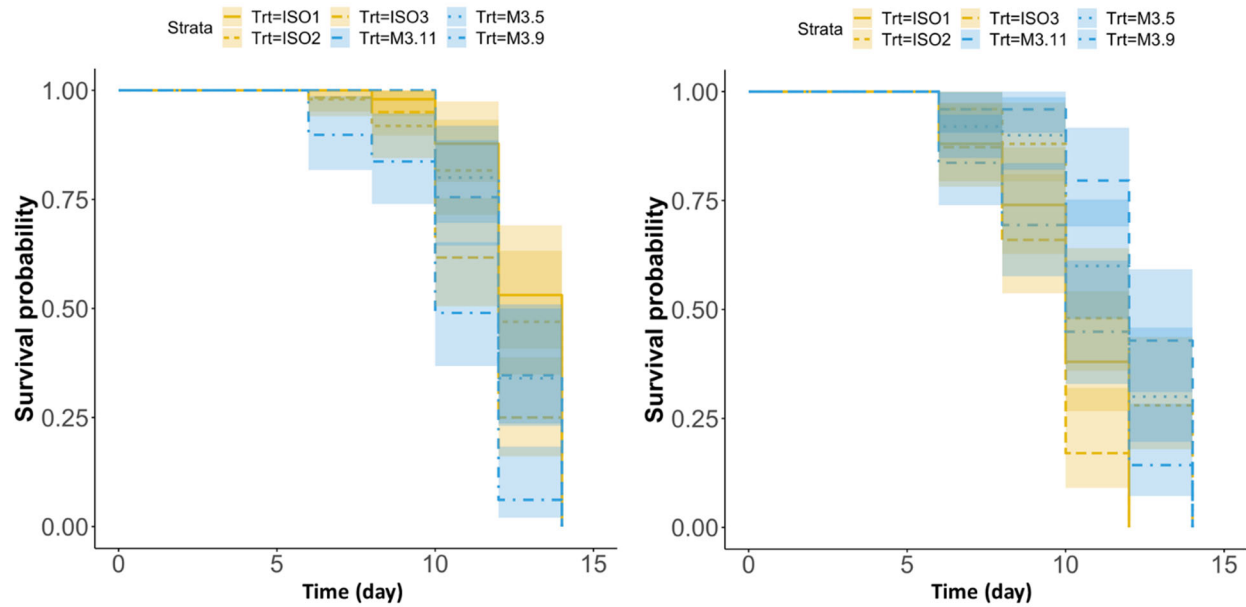


Figure S5. Knockout of the *mElo* orthologue *Gl20347* in *D. mojavensis* did not lead to significant differences in survival at 37°C in a non-desiccating environment. Differences in survival between the wild type and *Dmoj/mElo* knockout strains of *D. mojavensis* were determined using linear mixed model with the variation within each group (iso-female or independent knockout strains) being random effects. No significant differences were observed (Female: $P = 0.4$; Male: $P = 0.2$).

Figure S6. Phylogenetic tree of all elongases genes identified in *Drosophila melanogaster*, *Aedes aegypti*, *Apis mellifera*, *Bombyx mori*, and *Tribolium castaneum*. The elongase genes of each species is denoted with a different color. The tree showed that two elongases genes, *CG31523* and *sit*, have one-to-one orthologs across all five species. *mElo* is clustered with a few *Drosophila* genes suggesting that this gene is likely to be *Drosophila* specific.

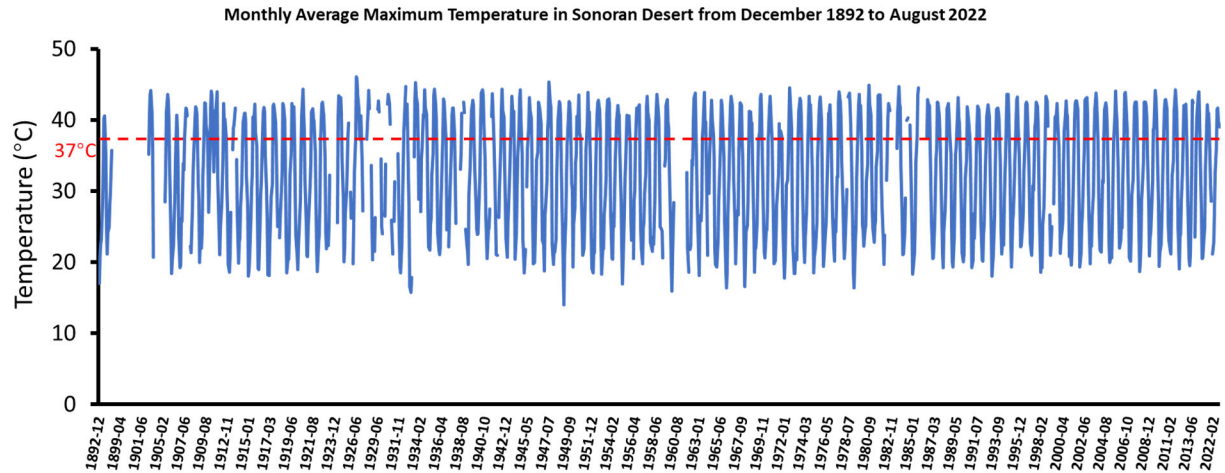


Figure S7. Monthly average maximum temperatures in the Sonoran Desert. Plot of monthly average maximum temperatures in a climatic station (GILA BEND 2 SE, AZ US) in the Sonoran Desert from December 1892 to August 2022. The climatic station is located at the coordinate 32.93803, -112.68109. The red dotted line indicates 37°C. The data were obtained from NCEI-NOAA (<https://www.nci.noaa.gov/>).

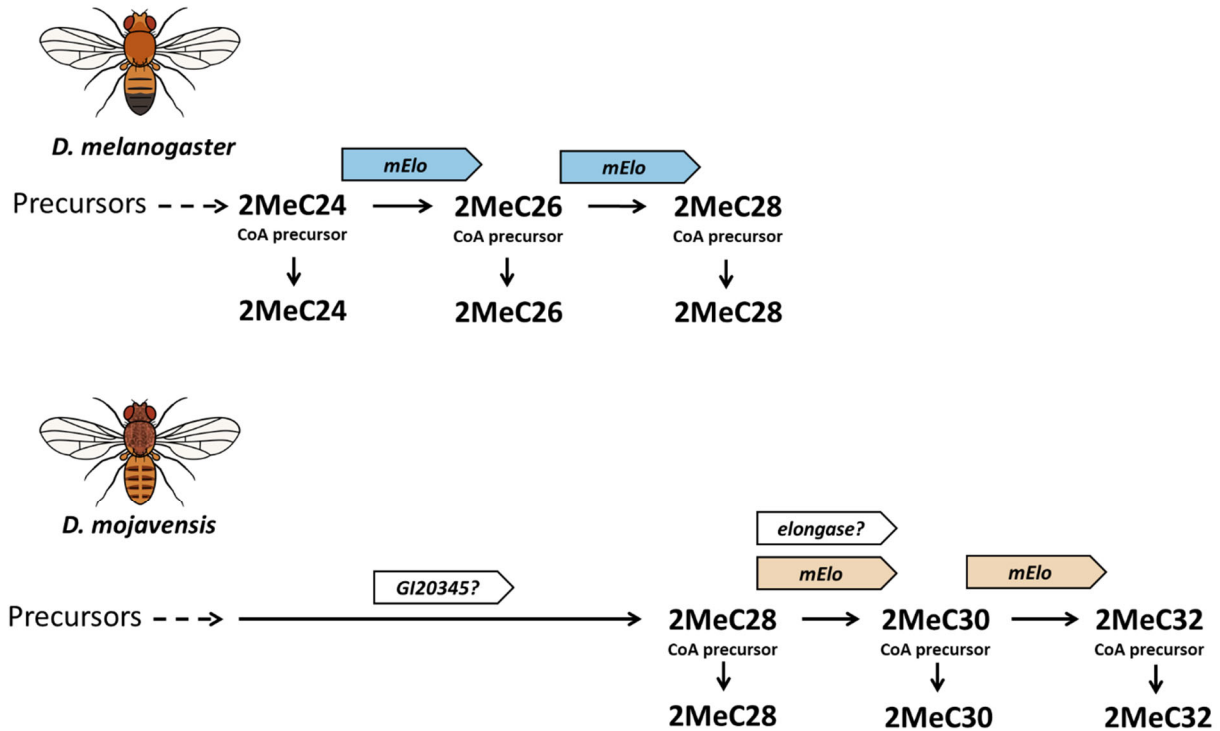


Figure S8. Model showing the production of mbCHCs in *D. melanogaster* and *D. mojavensis*. In *D. melanogaster*, the elongase *mElo* elongates 2MeC24 to 2MeC26 and 2MeC28. In the elongase *mElo* elongates 2MeC28 to 2MeC30 and 2MeC32, while elongation to 2MeC28 is due to another elongase, possibly *GI20345?*, which is expressed in *D. mojavensis* oenocytes and can elongate shorter mbCHCs to 2MeC28 when overexpressed in *D. melanogaster* oenocytes. As the knockout of *mElo* did not fully reduce the production of 2MeC30 in *D. mojavensis*, we hypothesize that another elongase may also be involved in the synthesis of mbCHCs up to 2MeC30 in *D. mojavensis*.

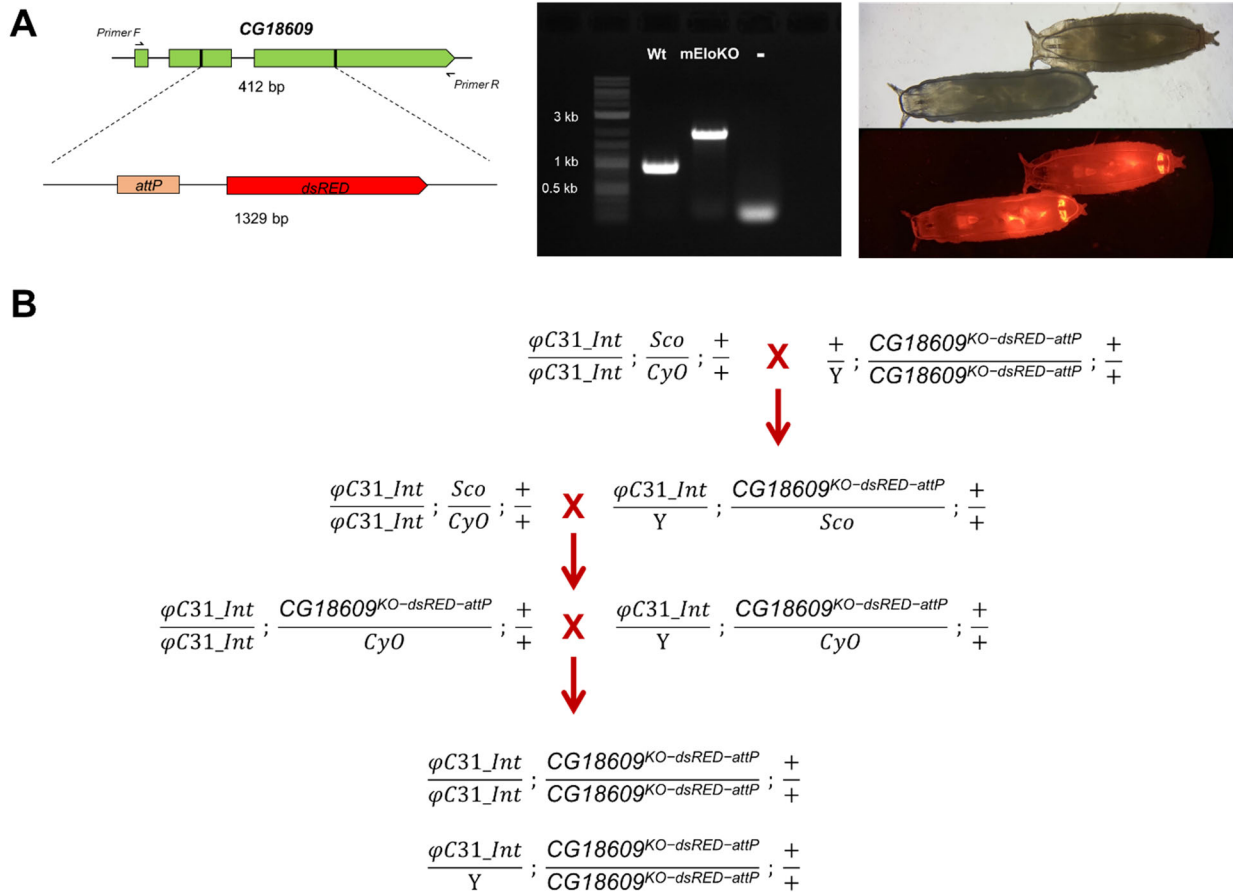


Figure S9. Generation of *mElo* knockout lines in *D. melanogaster*. A. Diagram of knockout using CRISPR/Cas9-mediated homology-directed repair on *Dmel/mElo* (Left panel). Successful knockout was confirmed with the replacement of the *attP/dsRED* sequence (Middle panel) as well as the presence of dsRed (Right panel). B. Crossing scheme to generate $w^{1118}, P\{y^{+17.7}=nos-phiC31\int int.NLS\}X; CG18609^{KO-dsRED-attP}$ (*mEloKOint*) strain.